Turbulence enhancement of stagnation point heat transfer on a body of revolution

G. K. Hargrave*, M. Fairweather*† and J. K. Kilham*

Enhancement, by free stream turbulence, of convective heat transfer to the stagnation region of a hemispherical-nosed cylinder has been studied. Increases in heat transfer were found to depend primarily on the Reynolds number and turbulence intensity of the free stream, experimental results being most successfully correlated on a $NuRe^{-0.5}$ versus $TuRe^{0.5}$ basis. Flow visualization studies have demonstrated the validity of a phenomenological model of the enhancement process, predictions of this theory showing good agreement with experimental results. The effect of free stream turbulence on the stagnation point velocity gradient has also been evaluated.

Keywords: *heat transfer, convection, turbulence, stagnation point, air flows*

Convective heat transfer to or from solid bodies immersed in a gas stream is important in many engineering situations, and it is now well established that the laminar boundary layer formed in the region of the stagnation point of a bluff body responds to free stream turbulence in such a way that heat transfer rates are increased. This effect has been demonstrated experimentally and quantified in terms of the turbulence properties of air streams for both circular cylinders[1,2] and spheres[3,4]. Theoretical treatments of the heat flux enhancement process have also appeared in the literature[5-7]. Amplification of vorticity due to the stretching of vortex filaments in the diverging flow near a stagnation point is now accepted as being responsible for this effect[8].

Turbulence enhancement of stagnation point heat transfer has also been reported recently for bodies of revolution (hemispherical-nosed cylinders) placed in both non-reacting[9] and reacting[9,10] turbulent flows, although the effect is reduced in the latter case. This type of heat-receiving body has frequently been used in heat transfer studies[9-11], and although vorticity amplification has been observed in the vicinity of the stagnation point of such bodies placed in turbulent air flow[12], no systematic study of the turbulence enhancement process has been made.

This paper examines in detail the enhancement process on a body of revolution placed in turbulent air flows.

Experimental

Flow visualization

The vorticity-amplification theory advanced by Sutera, Maeder and Kestin[8] suggests that turbulent fluctuations present in a free stream flow are susceptible to undergoing significant amplification as they are conveyed by a diverging mean flow towards the stagnation point of a body. Selective stretching of vortex filaments orientated laterally to the free stream direction was proposed as the mechanism responsible for the amplification of vorticity, and hence of free stream turbulence. The intensified turbulence is then considered to be the agent causing increases in shear stress and heat transfer at the surface of the body by inducing substantial three-dimensional effects in the stagnation point boundary layer.

Experimental verification of the vorticity-amplification theory for the two-dimensional flow around a circular cylinder was obtained by Sadeh, Sutera and Maeder[13] and later by Sadeh and Brauer[14]. Flow visualization studies by the latter authors confirmed the presence of selective stretching and streamwise biased tilting of vortex filaments in the diverging flow approaching a cylinder. These effects were seen to lead to the development of standing cross-vortex tubes distributed about the cylinder with their axes parallel to the streamlines around the body and with their cores outside the body boundary layer. Discrete vortices, or eddies, were also seen to be continuously drawn from this array of standing vortices, being swept downstream by the main flow while penetrating the body boundary layer and affecting its properties.

In order to permit the prediction of this enhancement effect from known free stream properties Smith and Kuethe[5], and later Galloway[6], employed a phenomenological theory based on the assumption that the random penetration of free stream eddies into the stagnation point boundary layer is responsible for increases in local transport and hence heat transfer rates. This theory was applied by Galloway[6] to stagnation point heat transfer on both cylinders and spheres, results indicating that the geometry of the bluff body has little effect on the enhancement process.

To obtain further justification for application of this approach to modelling the enhancement process, and in the absence of experimental information concerning the way in which free stream turbulence interacts with the

* Department of Fuel and Energy, The University, Leeds, UK
† Present address: British Gas Corporation, Midlands Research Station, Wharf Lane, Solihull, West Midlands, B91 2JW, UK
Received 29 October 1984 and accepted for publication on 17 December 1984

stagnation point boundary layer formed on a body of revolution, flow visualization studies were undertaken. These studies were performed using air jets issuing from a 500 mm long cylindrical tube with an internal diameter of 32 mm. The tube included a facility for introducing fine wire meshes close to the input nozzle in order to smooth out turbulence generated by the input pipes, and for placing various turbulence promoters in the vicinity of the exit nozzle. Three promoters in the form of perforated metal plates were used in the present study, these promoters generating exit flow turbulence intensities (measured by hot wire anemometry) of 0.013, 0.120 and 0.182. A mean exit flow velocity of 1 m/s was used in all tests. Because the flow visualization study sought to examine the enhancement process in the region of the stagnation point, a 100 mm diameter glass sphere painted with dead black lacquer was used as a bluff body for convenience. Flow visualization was carried out using titanium dioxide white smoke injected into the flow using a hypodermic tube. The flow rate through this tube was controlled in order to match the smoke exit velocity with the prevailing free stream value, thereby ensuring neutral entrainment. Monochrome cine films were taken of all tests using film speeds of 25 and 50 frames/s.

Stagnation point velocity gradient

The stagnation point velocity gradient β is an aerodynamic parameter which describes the flow just outside the boundary layer of a body by defining the velocity gradient in the mean flow as it moves away from the stagnation point around the body. This parameter is an essential input to theoretical models of stagnation point heat transfer.

In the absence of any experimental determination of β for hemispherical-nosed cylinders, stagnation point heat transfer to such bodies from both laminar[11,15] and turbulent[10] free streams has previously been predicted on the basis of values derived for a sphere placed in a laminar flow. For the case of incompressible laminar flow around a sphere therefore, potential flow theory gives β as a simple function of free stream velocity and sphere diameter[16]. Conolly and Davies[15] assessed the applicability of values derived in this way to a hemispherical-nosed cylinder placed in a laminar free stream, results indicating a maximum discrepancy of 4% between measured heat transfer coefficients and predictions.

Donaldson *et al.*[17,18] measured the velocity gradient parameter in the stagnation region of a 152 mm diameter hemispherical body immersed in an air jet from a 13 mm diameter nozzle, results indicating that β varied significantly with increasing distance downstream of the nozzle. Hot wire measurements of the air jet flow further revealed β to be a function of free stream turbulence intensity as well as velocity. Van der Meer and Hoogendoorn[19] also noted the influence of turbulence intensity on β for heat transfer from premixed jet flames impinging on a flat plate. These authors had some success in allowing for the enhancement effect of free stream turbulence by predicting heat transfer rates using the laminar theory of Sibulkin[16], modified using an experimentally determined velocity gradient parameter.

To obtain values of β applicable to the hemispherical-nosed cylinder geometry, and to investigate the influence of free stream turbulence on this parameter, static pressure measurements were taken on the surface of such a body placed in a turbulent air flow. The static pressure distribution in the immediate vicinity of the stagnation point was then used to derive values of the velocity gradient parameter. The probe used in these experiments consisted of a 22 mm diameter hollow brass hemispherical-nosed body with ten pressure tappings arranged in a spiral formation centering on the stagnation point. The pressure tappings were made from stainless steel hypodermic tubing of 0.8 mm inner diameter, fixed flush with the outer surface of the hemispherical section of the probe. Each hypodermic tube was connected using narrow bore PTFE tubing to a ten way manifold which

Notation

a	Defined in Eq (9)
D	Diameter of hemispherical-nosed cylinder
f'	Ratio of u at a point in boundary layer to value at boundary layer outer edge
G	Mass velocity
k	Constant defined in Eq (4)
K	Defined in Eq (17)
Nu	Nusselt number
p	Pressure
Pr	Prandtl number
Re	Reynolds number
Re_T	Turbulent Reynolds number
St	Stanton number
T	Temperature
Tu	Turbulence intensity
u	Velocity component in x direction
v	Velocity component in y direction
x	Distance along surface of axisymmetric body from stagnation point
y	Distance perpendicular to surface of axisymmetric body through boundary layer
α	Thermal diffusivity
β	Stagnation point velocity gradient
ε	Momentum and thermal eddy diffusivity
η	Transformed y coordinate
θ	Defined by Eq (8)
μ	Dynamic viscosity
ν	Kinematic viscosity
ρ	Density
ψ	Stream function

Subscripts

e	Evaluated at outer edge of boundary layer
local	Local value
w	Evaluated at body surface
∞	Free stream value

Superscripts

$'$	Differentiation with respect to η

allowed the switching of each individual tapping to a micromanometer.

Isothermal air jets were generated using the 32 mm diameter cylindrical tube employed in the flow visualization study, and an equivalent 16 mm diameter tube. Five perforated metal plate turbulence promoters were used with the 32 mm diameter nozzle, two promoters being used with the smaller diameter tube. Exit turbulence intensities and mean flow velocities over the ranges 0.018–0.180 and 2.75–10.00 m/s, and 0.070–0.110 and 5.0–20.0 m/s, were obtained using the larger and smaller nozzle diameters respectively.

In conducting these experiments the pressure probe was clamped in a fixed position, and the cylindrical tubes mounted on a two-axis traverse allowing the exit nozzle to be positioned axially and radially relative to the probe. Axial and radial free stream velocities were measured using laser Doppler anemometry (LDA). The system was of a dual-beam, forward scatter design, utilising a 2 W argon ion laser. The flow was seeded with alumina particles of 1 μm mean diameter using a fluidised bed cyclone device[20].

Convective heat transfer from heated air jets

Convective heat transfer to the hemispherical-nosed cylinder geometry was studied using heated air jets issuing from the 16 mm diameter cylindrical tube used for stagnation point velocity gradient measurements. Four turbulence promoters were used in conjunction with this tube, generating exit turbulence intensities over the range 0.012–0.230. Mean exit flow velocities of 12–16 m/s were employed. Heated air was supplied using a series of electrical heating elements producing a mean temperature of approximately 600 K through the exit nozzle of the tube. A means of seeding this air was also included to facilitate free stream velocity measurements using the LDA system.

A steady state calorimeter[21] (Fig 1) was constructed for the measurement of heat flux at the stagnation point of a 22 mm diameter hemispherical-nosed body. In this device a 3.2 mm diameter copper rod was exposed to hot air flows at the stagnation point of the probe, the main body of which was maintained at 373 K using glycol. The other end of the copper rod was cooled with a controlled water flow. Four thermocouples were attached along the length of the rod. One measured the temperature of the exposed surface, a second the cold end temperature, and two others were positioned at a known separation along the rod. The heat flux at the stagnation point of the probe was then determined from measured temperature differences and the thermal properties of copper. In order to avoid any inaccuracies arising from unpredictable heat losses, the calorimeter was also calibrated with known heat fluxes from a black-body furnace.

Temperatures along the axis of an air jet were measured using a pre-calibrated micro-suction pyrometer. Radial temperatures were determined by the use of fine wire chromel-alumel thermocouples.

Theory

The boundary layer equations for incompressible flow with constant properties near the stagnation point of a body of revolution may be written as:

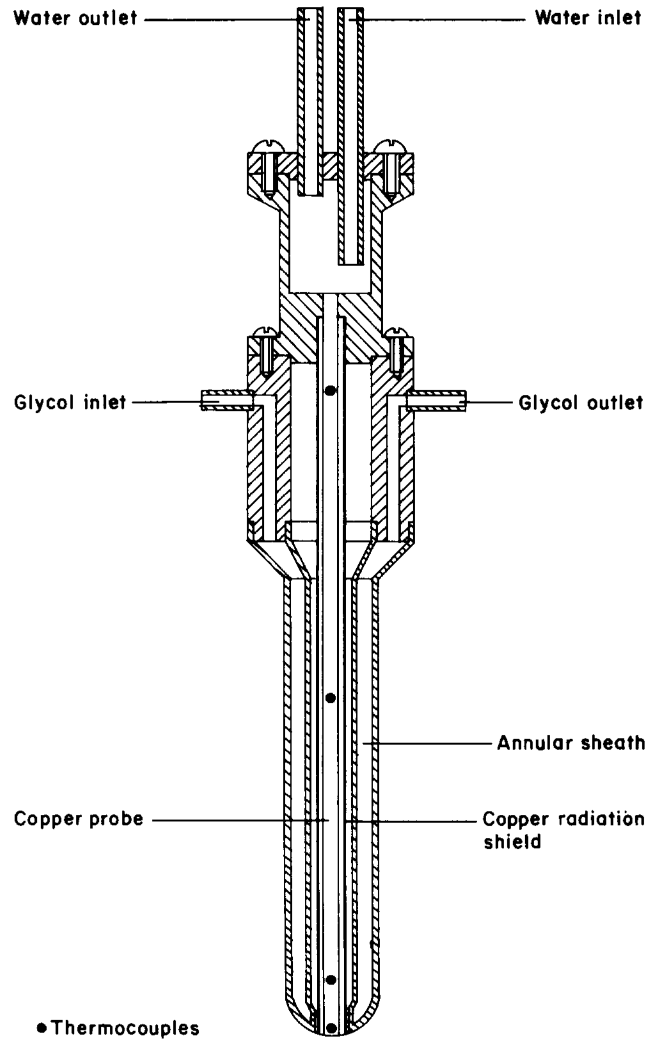

Fig 1 Steady state calorimeter

$$\frac{\partial(ux)}{\partial x}+\frac{\partial(vx)}{\partial y}=0 \tag{1}$$

$$\frac{u\partial u}{\partial x}+\frac{v\partial u}{\partial y}=-\frac{1}{\rho}\frac{\partial p}{\partial x}+\frac{\partial}{\partial y}\left((v+\varepsilon)\frac{\partial u}{\partial y}\right) \tag{2}$$

$$\frac{u\partial T}{\partial x}+\frac{v\partial T}{\partial y}=\frac{\partial}{\partial y}\left((\alpha+\varepsilon)\frac{\partial T}{\partial y}\right) \tag{3}$$

In these equations ε is the momentum and thermal eddy diffusivity, implying a turbulent Prandtl number of unity. The purpose of employing an eddy diffusivity is one of convenience, to accommodate the complexities of the enhancement process in the vicinity of the stagnation point in a single term. The eddy law itself may then be formulated in such a way as to describe the enhancement of transport in a laminar boundary layer with imposed perturbations.

After Smith and Kuethe[5], and Galloway[6], homogeneous and isotropic free stream turbulence is assumed and Prandtl's mixing length concept used in order to derive an eddy law. The turbulence intensity of the free stream defined at a reference position in the flow field corresponding to the bluff body stagnation point with the body removed is then taken to be the external driving force which sets the level of velocity fluctuations in the boundary layer near the stagnation point. Thus, as the fluctuating components penetrate into the laminar boundary layer from the turbulent free stream, the fluctuating velocity is expected to be proportional to the external free stream turbulence and flow conditions. The resulting eddy law may be written as:

$$\varepsilon = \mathrm{k} Tu_{\infty} u_{\infty} y, \tag{4}$$

where k is a constant to be determined from experimental data.

Proceeding with the analysis, a stream function ψ is defined such that $u=(1/x)\partial\psi/\partial y$ and $v=-(1/x)\partial\psi/\partial x$, these expressions satisfying the continuity equation automatically. Defining

$$u_e = \beta x \tag{5}$$

$$\psi = (v\beta)^{0.5} x^2 f(\eta) \tag{6}$$

$$\eta = (\beta/v)^{0.5} y \tag{7}$$

$$\theta = \frac{T_w - T(\eta)}{T_w - T_{\infty}} \tag{8}$$

$$a = \frac{1}{3^{0.5}} \mathrm{k} Tu_{\infty} Re_{\infty}^{0.5} \tag{9}$$

and substituting these expressions into Eqs (2) and (3), the transformed momentum and energy equations may be written as:

$$f'''(1+a\eta) + 2f''\left(f + \frac{a}{2}\right) + (1-(f')^2) = 0 \tag{10}$$

$$\theta'' + \frac{\theta'(2f+a)}{\left(a\eta + \frac{1}{Pr}\right)} = 0, \tag{11}$$

where prime denotes differentiation with respect to η. The transformed boundary conditions are:

$$f(0) = f'(0) = 0 \quad \text{and} \quad f'(\infty) = 1 \tag{12}$$

$$\theta(0) = 0 \quad \text{and} \quad \theta(\infty) = 1. \tag{13}$$

Eqs (10) and (11) were solved using Merson's method in conjunction with a Newton iteration in a shooting and matching technique[22]. The variation of $NuRe^{-0.5}$ with chosen values of k and $TuRe^{0.5}$ in Eq (9) was then obtained from:

$$NuRe^{-0.5} = 3^{0.5}\theta'(0), \tag{14}$$

where in determining this dependence it is necessary to assume a constant value of $\beta = 3u_{\infty}/D$ after Sibulkin[16].

Predictions of a model equivalent to that described above, but which allows for density and property variations through the boundary layer and for the dependence of β on free stream turbulence, have also been used in the present study. This model is described in detail elsewhere[10].

Finally, predictions have been made on the basis of Sibulkin's equation[16] derived from numerical solutions of the laminar boundary layer equations. Applicable to constant property incompressible flow conditions, this equation may be written as:

$$St = 0.763 G^{-1} Pr^{-0.6} (\beta \rho_e \mu_e)^{0.5}, \tag{15}$$

or after rearranging:

$$NuRe^{-0.5} Pr^{-0.4} = 0.763\left(\frac{\beta D}{u_{\infty}}\right)^{0.5} \tag{16}$$

Following the approach of Van der Meer and Hoogendoorn[19], the enhancement effect of free stream turbulence was incorporated into this expression using experimentally determined values of the velocity gradient parameter.

Results and discussion

Flow visualization

Visualization studies using a low turbulence intensity (0.013) revealed the essentially laminar nature of the flow field. Streamlines approaching the body were generally smooth, with the flow diverging evenly at the stagnation point and the body boundary layer being clearly defined. Despite the flow being substantially laminar, however, some unsteadiness was noted near the stagnation point.

Results typical of those obtained using an exit flow turbulence intensity of 0.12 are shown in Fig 2. This figure contains eight representative frames taken from the cine films obtained, together with sketches of the flow patterns observed. The nozzle exit velocity employed in all tests corresponds to a laminar boundary layer thickness[23] of approximately 1.4 mm on the body of revolution.

In a similar way to studies performed using circular cylinders[14], the first three frames in this figure show the development of a vortex in the vicinity of the stagnation point. From 83–125 ms the vortex remains stable, having grown to 8–10 mm in diameter. At 167 ms

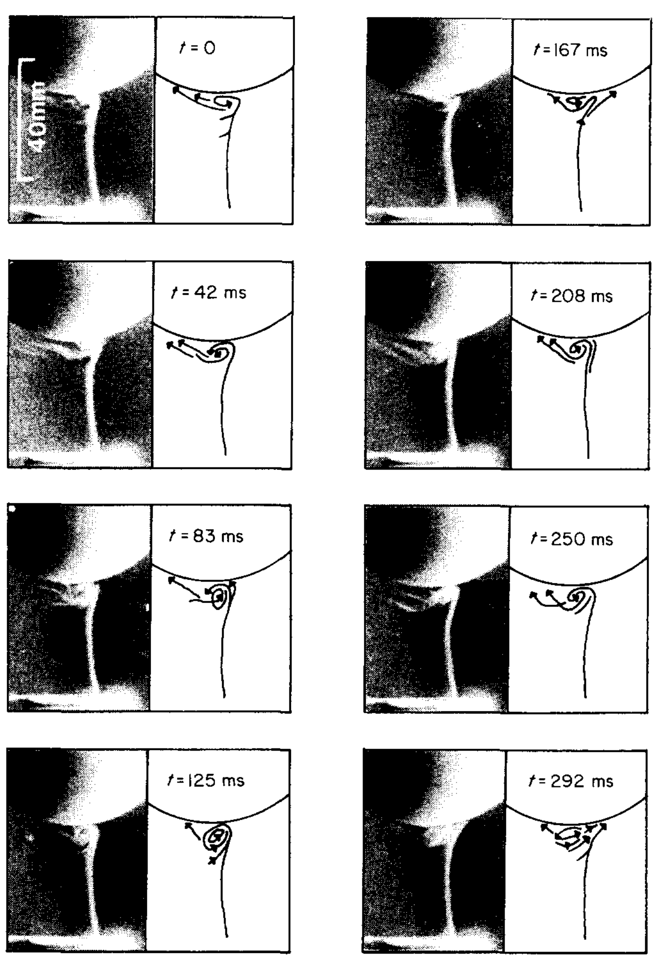

Fig 2 Flow visualization using an exit flow turbulence intensity of 0.12

the vortex suddenly breaks up and the flow at the stagnation point becomes random. This is rapidly followed by the redevelopment of another vortex which remains stable for 50–60 ms, the flow again becoming random in the last frame of Fig 2. An overall examination of many seconds of cine film revealed this sequence of events to be typical of the flow field studied. Vortices at the stagnation point therefore existed for relatively short periods, of the order of 100 ms, with the stagnation flow randomly becoming irregular with varying streamlines around the body. It was also noted that the break up of a vortex was often accompanied by the creation of spiral formations, similar in appearance to those observed by Sadeh and Brauer[14]. Thus, as a vortex passed from the stagnation region through the accelerating flow around the body it was pulled out into a helix-like spiral aligned with the streamlines around the body.

Cine films of the high turbulence intensity (0.182) flow were difficult to interpret because of the rapid flow velocity fluctuations, turbulence breaking up the smoke filaments so rapidly in the flow approaching the body that the smoke was too diffuse to scatter sufficient light for photographic purposes. In general, however, the flow field observed was qualitatively similar to that discussed above.

Overall it may be concluded that, unlike the relatively stable cross-vortex tubes formed in the stagnation region of cylinders placed in turbulent flows[14], the stagnation flow on a sphere exhibits a more unstable and irregular flow structure with the formation of short-lived vortices.

Stagnation point velocity gradient

Axial and radial profiles of mean velocity and turbulence intensity typical of an air jet issuing from the 32 mm diameter nozzle are presented in Fig 3. To eliminate the effect of varying radial velocities, all pressure measurements in air jets from both the 16 and 32 mm nozzles were made at positions downstream which exhibited a substantially flat velocity profile over at least 80% of the diameter of the hemispherical-nosed probe.

Measured pressure distributions around the probe were converted to local free stream velocities using Bernoulli's equation. Increases in local velocity as the flow moved away from the stagnation point were found to be linear in the stagnation point region, the effect of turbulence in increasing the velocity gradient at the stagnation point being readily apparent in derived velocity profiles.

To accommodate the effect of free stream turbulence in increasing the stagnation point velocity gradient, β may be defined as:

$$\beta = \frac{K u_\infty}{D} \quad (17)$$

by analogy with expressions derived from potential flow theory. The parameter K is now assumed to be a function of turbulence intensity. Values of K were obtained directly from plots of the measured non-dimensionalised velocity gradient $d(u_{local}/u_\infty)/d(x/D)$ in the vicinity of the stagnation point. The dependence of this parameter on turbulence intensity determined in this way is shown in Fig 4(a), results being based on mean free stream velocities and turbulence intensities over the ranges 2.5–20.0 m/s and

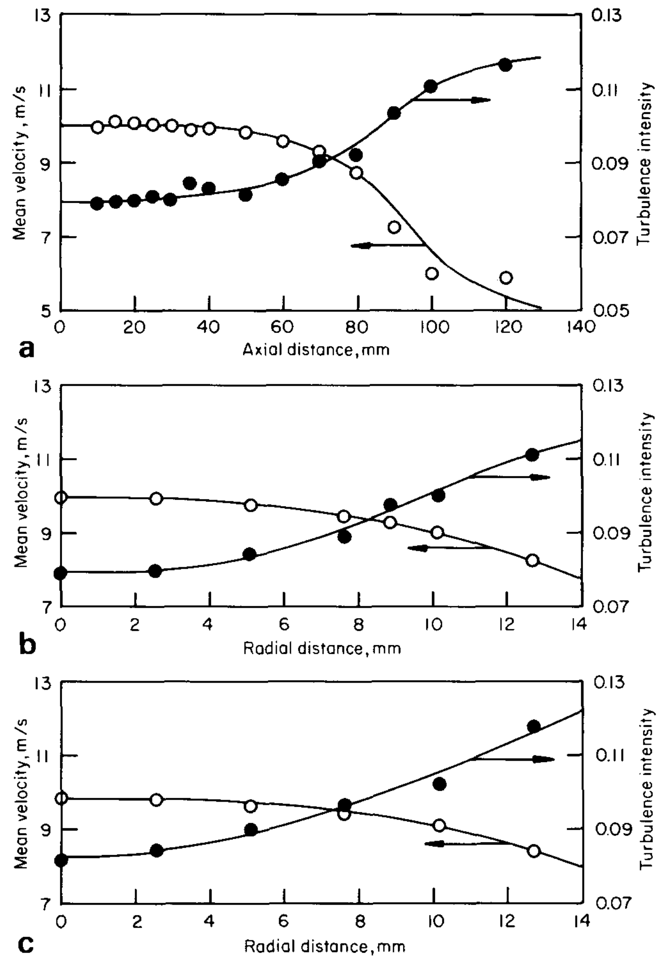

Fig 3 Typical mean velocity and turbulence intensity profiles for an isothermal air jet issuing from the 32 mm diameter nozzle. (a) Axial variation, and radial variation at (b) 10 mm downstream and (c) 50 mm downstream

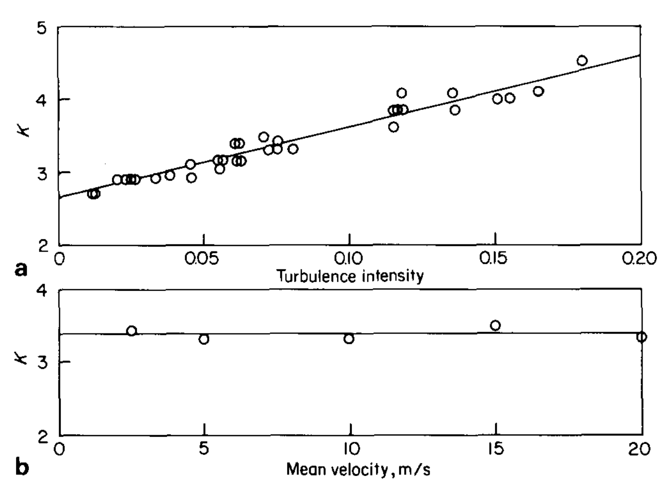

Fig 4 Variation of velocity gradient parameter K with (a) turbulence intensity and (b) mean velocity

0.012–0.180 respectively. A least squares fit to this data yields:

$$K = 2.67 + 9.62 Tu_\infty, \quad (18)$$

where a value of 2.67 is obtained for the case of a laminar free stream flow. This is in good agreement with the experimental value of 2.66 obtained by Newman, Sparrow and Eckert[24] for an essentially laminar flow ($Tu_\infty = 0.002$–0.003) about a sphere, and compares with a theoretical value of 3 obtained from potential flow theory[16]. The invariance of K with mean free stream velocity is illustrated in Fig 4(b), data given in this plot having been obtained at turbulence intensities between 0.07 and 0.08.

Convective heat transfer from heated air jets

The structure of a typical hot air jet issuing from the 16 mm diameter nozzle is shown in Figs 5 and 6. All heat flux measurements were again made in regions of the jets which exhibited substantially flat radial profiles of mean velocity, turbulence intensity and temperature over a significant proportion of the diameter of the heat receiving body.

In a similar manner to the data obtained by Gostkowski and Costello[4] for spheres, these stagnation point heat flux results were found to correlate for a particular free stream Reynolds number when plotted in terms of $NuRe^{-0.5}$ versus Tu. Heat transfer results were therefore dependent primarily on the mean free stream velocity, or Reynolds number, and turbulence intensity. Reducing the data in terms of a turbulent Reynolds number results in the plot shown in Fig 7. The non-dimensional parameters in this figure are based on mean free stream velocities and turbulence intensities, the diameter of the hemispherical portion of the heat flux

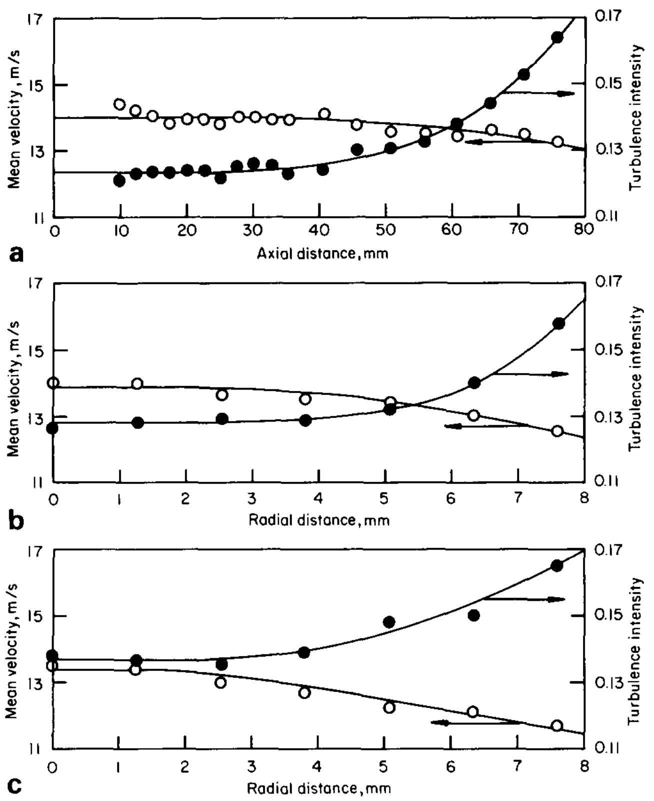

Fig 5 Typical mean velocity and turbulence intensity profiles for a heated air jet issuing from the 16 mm diameter nozzle. (a) Axial variation, and radial variation at (b) 30.3 mm downstream and (c) 60.8 mm downstream

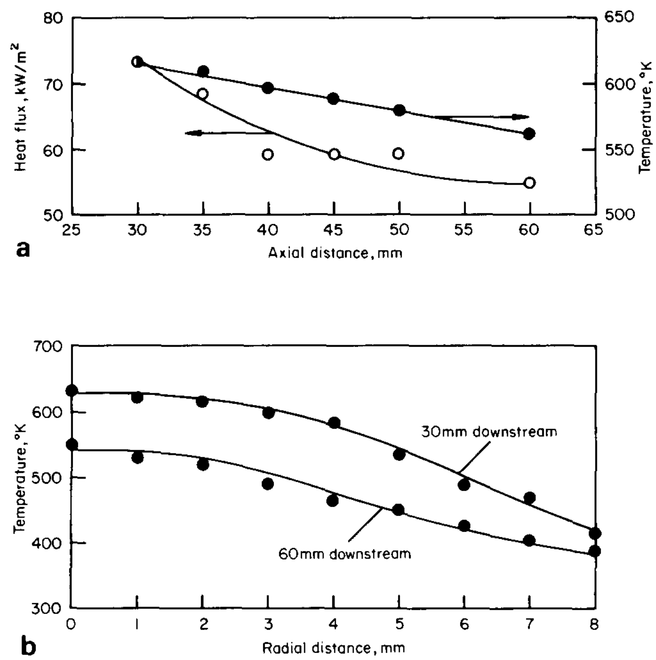

Fig 6 Variation of (a) axial heat flux and temperature and (b) radial temperature for the heated air jet described in Fig 4

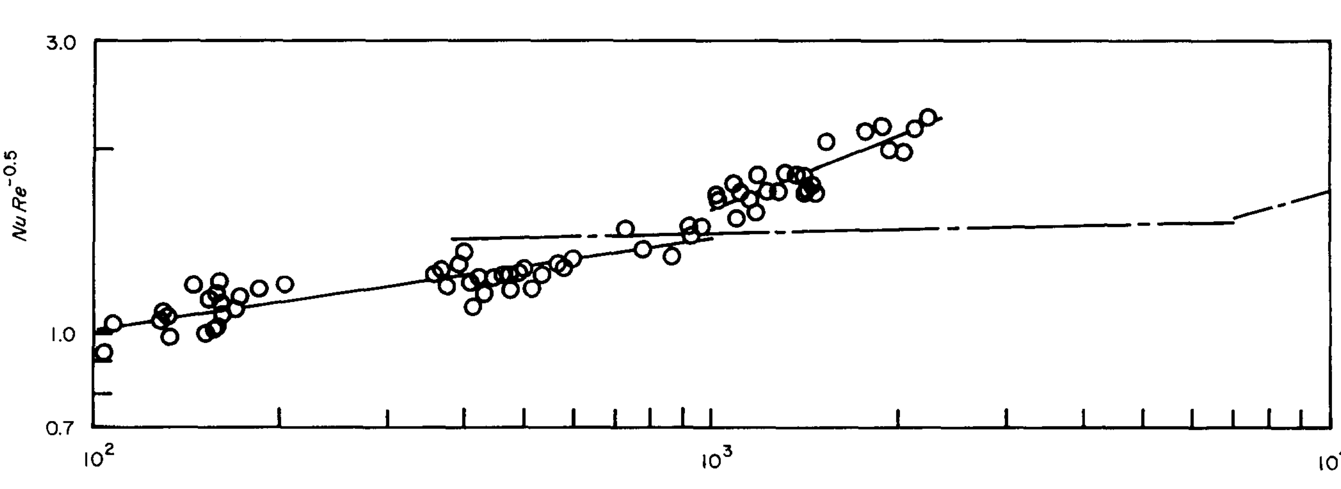

Fig 7 Heat flux data expressed as variation of $NuRe^{-0.5}$ *with* TuRe (○ *experimental, —— fitted, – – – Ref 4*)

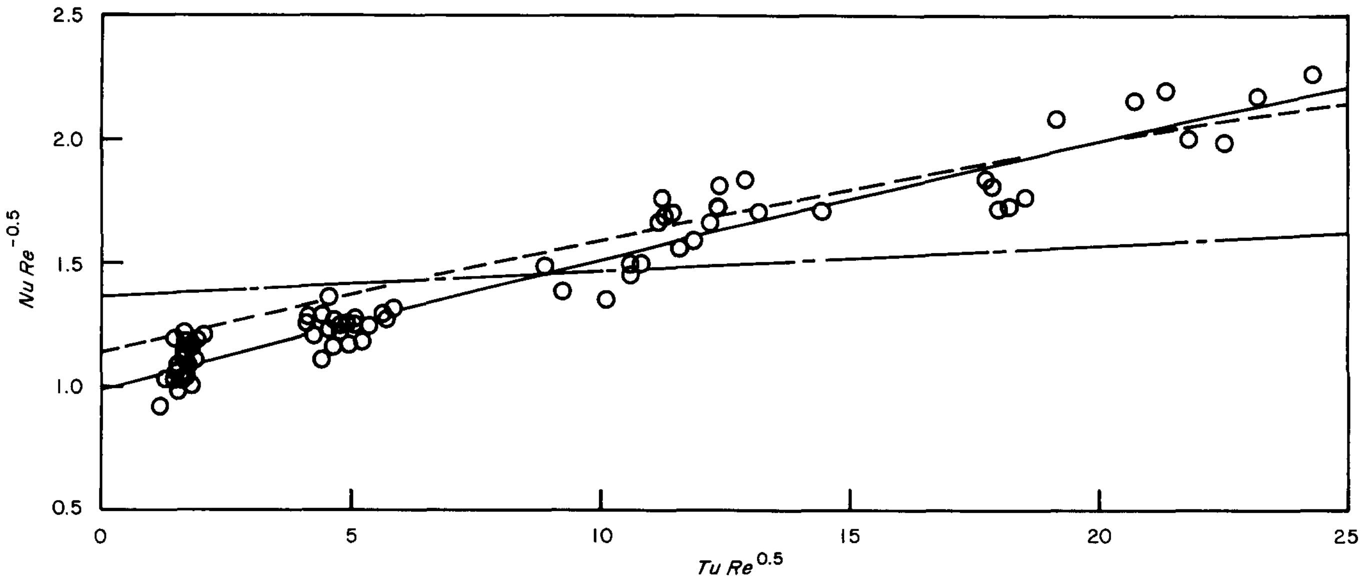

Fig 8 Heat flux data expressed as variation of $NuRe^{-0.5}$ *with* $TuRe^{0.5}$ *(○ experimental, —— fitted, — — — Ref 4, - - - numerical solution)*

probe, and on air properties evaluated at the mean boundary layer temperature.

The results given in this figure show that the relation between $NuRe^{-0.5}$ and Re_T is essentially linear in the low turbulent Reynolds number range, with a sharp increase in heat flux occurring in the vicinity of $Re_T = 1000$; for $NuRe^{-0.5}$ and Re_T based on air properties evaluated at the free stream temperature, this transition occurs at $Re_T = 700$. Lavender and Pei[25] observed a similar increase in macroscopic heat transfer from a sphere at $Re_T = 1000$, and the data of Smith and Kuethe[5] for heat transfer from the stagnation line of a cylinder exhibits a transition at the same turbulent Reynolds number. The stagnation point heat flux data obtained by Gostkowski and Costello[4] for a heated sphere placed in turbulent air flows is also in qualitative agreement with these findings, although the transition to higher heat transfer rates was found to occur at $Re_T = 7000$. Least squares fits to the data of the latter authors are shown in Fig 7. A possible explanation of this shift in transition point, suggested by Gostkowski and Costello, is that it may be dependent on the actual free stream velocity and turbulence intensity ranges studied.

A number of workers have achieved a more successful correlation of experimental data on the basis of $NuRe^{-0.5}$ versus $TuRe^{0.5}$ values, the present data being shown in this form in Fig 8. A least squares fit to this data gives:

$$NuRe^{-0.5} = 0.993 + 5.465\left(\frac{TuRe^{0.5}}{100}\right) - 2.375\left(\frac{TuRe^{0.5}}{100}\right)^2 \quad (19)$$

valid over the ranges $0.014 \leqslant Tu \leqslant 0.267$, $5855 \leqslant Re \leqslant 10492$ and $8.73\ \text{m/s} \leqslant u_\infty \leqslant 16.25\ \text{m/s}$. For comparison, a least squares fit to the sphere data of Gostkowski and Costello[4] is also shown in Fig 8. From both Figs 7 and 8, results of the latter authors are seen to overestimate the present data at low Re_T and $TuRe^{0.5}$ values and to underestimate that data at higher Re_T and $TuRe^{0.5}$.

Predictions of the phenomenological theory described earlier are also given in Fig 8, these results having been derived using a Prandtl number for air evaluated at a mean boundary layer temperature averaged over all the experimental tests. The fitted curve shown was obtained assuming k = 0.284 in the eddy law defined by Eq (4). This value compared with 0.164 and 0.1 evaluated by Smith and Kuethe[5] and Galloway[6] respectively for heat transfer from the stagnation line of a circular cylinder. It may be noted that for the case of a laminar free stream, predictions of this theory and Eq (19) agree well with the laminar theory of Sibulkin[16] which gives $NuRe^{-0.5} = 1.07$ (ie Eq (16) with $\beta = 2.67u_\infty/D$ and an averaged Pr for air).

Because of the large temperature differences across the stagnation point boundary layer present in the flows examined, the constant k was also evaluated using a compressible model[10] and expressing β as a function of free stream turbulence intensity according to Eqs (17) and (18). Fitting of the experimental data was accomplished by calculating average mean free stream velocities, turbulence intensities and temperature differences across the boundary layer for each exit velocity and turbulence promoter used in the experiments. Comparison with experimental data was then made on a heat flux basis, and a value of k = 0.2 derived as the best fit.

Finally, Fig 9 shows predictions of Eq (16) derived using a variable stagnation point velocity gradient, according to Eqs (17) and (18), for free streams with turbulence intensities less than 0.15. Although this method of allowing for the enhancement effect of free stream turbulence in the laminar theory results in an underprediction of heat transfer rates in high turbulence intensity flows, reasonable agreement with experiment is found at low turbulence intensities. This simple prediction method has in fact been applied with some success to heat transfer from low turbulence intensity non-reacting and combusting flows[9].

Conclusions

Flow visualization studies have demonstrated the unstable and irregular flow structure formed in the stagnation point region of a body of revolution placed in a

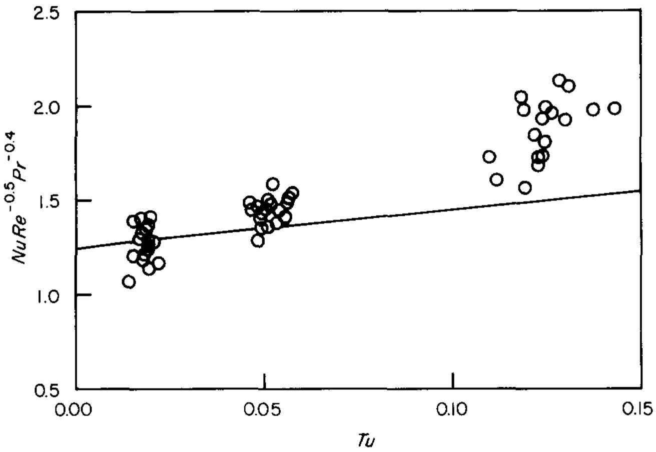

Fig 9 Heat flux data expressed as variation of $NuRe^{-0.5}Pr^{-0.4}$ *with* Tu (○ *experimental*, — *Eq (16)*)

turbulent free stream. The formation of relatively short-lived vortices at the stagnation point, and their interaction with the body boundary layer in this region, supports use of the phenomenological random eddy penetration theory for predicting the enhancement of stagnation point heat transfer by free stream turbulence.

The stagnation point velocity gradient, an essential input to theoretical models of stagnation point heat transfer, has been evaluated for a hemispherical-nosed cylinder as a function of free stream turbulence intensity. For the case of a laminar free stream, extrapolation of the present experimental results yields a value of this parameter in close agreement with theoretical and experimental evaluations for the case of a sphere.

Experimental measurements of convective heat transfer rates to a hemispherical-nosed cylinder indicate that the local heat flux in the stagnation point region is sensitive to turbulence in the free stream flow. Increases in heat transfer were dependent on the Reynolds number and turbulence intensity of the free stream, the relationship between $NuRe^{-0.5}$ and Re_T, and between $NuRe^{-0.5}$ and $TuRe^{0.5}$, adequately correlating heat transfer measurements. Predictions of a phenomenological theory of the enhancement process show good agreement with experimental results.

Acknowledgement

The authors would like to thank the British Gas Corporation for financing this project and for permission to publish.

References

1. **Galloway T. R. and Sage B. H.** Local and macroscopic transport from a 1.5 in cylinder in a turbulent air stream. *A.I.Ch.E.J., 1967*, **13**, *563–570*
2. **Lowery G. W. and Vachon R. I.** The effect of turbulence on heat transfer from heated cylinders. *Int. J. Heat Mass Transfer, 1975*, **18**, *1229–1242*
3. **Galloway T. R. and Sage B. H.** Thermal and material transfer from spheres, prediction of local transport. *Int. J. Heat Mass Transfer, 1968*, **11**, *539–549*
4. **Gostkowski V. J. and Costello F. A.** The effect of free stream turbulence on the heat transfer from the stagnation point of a sphere. *Int. J. Heat Mass Transfer, 1970*, **13**, *1382–1386*
5. **Smith M. C. and Kuethe A. M.** Effects of turbulence on laminar skin friction and heat transfer. *Physics Fluids, 1966*, **9**, *2337–2344*
6. **Galloway T. R.** Enhancement of stagnation flow heat and mass transfer through interactions of free stream turbulence. *A.I.Ch.E.J., 1973*, **19**, *608–617*
7. **Gorla R. S. R.** Influence of turbulence intensity and free stream velocity oscillations on stagnation point heat transfer. *Int. J. Heat Fluid Flow, 1982*, **3**, *195–200*
8. **Sutera S. P., Maeder P. F. and Kestin J.** On the sensitivity of heat transfer in the stagnation point boundary layer to free-stream vorticity. *J. Fluid Mech., 1963*, **16**, *497–520*
9. **Hargrave G. K. and Kilham J. K.** The effect of turbulence intensity on convective heat transfer from premixed methane-air flames. *Proc. First UK National Conference on Heat Transfer, Inst. Chem. Engs. Symp. Series No. 86, 1984, 1025–1034*
10. **Fairweather M., Kilham J. K. and Mohebi-Ashtiani A.** Stagnation point heat transfer from turbulent methane-air flames. *Combustion Science and Technology, 1984*, **35**, *225–238*
11. **Fairweather M., Kilham J. K. and Nawaz S.** Stagnation point heat transfer from laminar, high temperature methane flames. *Int. J. Heat Fluid Flow, 1984*, **5**, *21–27*
12. **Kuethe A. M., Willmarth W. W. and Crocker G. H.** Stagnation point fluctuations on a body of revolution. *Physics Fluids, 1959*, **2**, *714–716*
13. **Sadeh W. Z., Sutera S. P. and Maeder P. F.** An investigation of vorticity amplification in stagnation flow. *ZAMP, 1970*, **21**, *717–742*
14. **Sadeh W. Z. and Brauer H. J.** A visual investigation of turbulence in stagnation flow about a circular cylinder. *J. Fluid Mech., 1980*, **99**, *53–64*
15. **Conolly R. and Davies R. M.** A study of convective heat transfer from flames. *Int. J. Heat Mass Transfer, 1972*, **15**, *2155–2172*
16. **Sibulkin M.** Heat transfer near the forward stagnation point of a body of revolution. *J. Aero. Sci., 1952*, **19**, *570–571*
17. **Donaldson C. DuP. and Snedeker R. S.** A study of free jet impingement. Part 1. Mean properties of free and impinging jets. *J. Fluid Mech., 1971*, **45**, *281–319*
18. **Donaldson C. DuP., Snedeker R. S. and Margolis D. P.** A study of free jet impingement. Part 2. Free jet turbulent structure and impingement heat transfer. *J. Fluid. Mech., 1971*, **45**, *477–512*
19. **Van der Meer Th. H. and Hoogendoorn C. J.** Turbulent heat transfer on a plane surface of impinging round premixed flame jets. *Int. Flame Res. Foundation, Proc. Fifth Members Conference, 1978, 149–170*
20. **Glass M. and Kennedy I. M.** An improved seeding method for high temperature laser Doppler velocimetry. *Combustion and Flame, 1977*, **29**, *333–335*
21. **Cookson R. A. and Kilham J. K.** Energy transfer from hydrogen-air flames. *Ninth Symposium (International) on Combustion, 1963, 257–263*
22. *Numerical Algorithms Group, Nag Library Manual Mark 8, Volume 1, 1981*
23. **Schlichting H.** Boundary Layer Theory. *McGraw-Hill, 1960*
24. **Newman L. B., Sparrow E. M. and Eckert E. R. G.** Free-stream turbulence effects on local heat transfer from a sphere. *J. Heat Transfer, 1972*, **94**, *7–16*
25. **Lavender W. J. and Pei C. T.** The effect of fluid turbulence on the rate of heat transfer from spheres. *Int. J. Heat Mass Transfer, 1967*, **10**, *529–539*